Article ID: 1007-4627(2023) 00-0001-08

Anisotropic emission from magnetized quark-gluon plasma

Xiaozhu Yu[1], Xinyang Wang[1]

(*1. Department of Physics, Jiangsu University, Zhenjiang 212013, China*)

Abstract: In these proceedings, the polarization effects of a strongly magnetized quark-gluon plasma are studied at finite temperature. It is found that a background magnetic field can have a strong effect on the photon and dilepton emission rates. It affects not only the total rate but also the angular dependence. In particular, the Landau-level quantization leads to a nontrivial momentum dependence of the photon/dilepton ellipticity coefficient on transverse momentum. It is proposed that the anisotropy of the photon and dilepton emission may serve as indirect measurements of the magnetic field.

Key words: heavy ion collision; electromagnetic probes; strong magnetic field; finite temperature theory;
CLC number: 0000.0 **Document code:** A **DOI:** 10.11804/NuclPhysRev.00.01.01

1 Introduction

There has been a growing interest in the properties of Quantum chromodynamics (QCD) matter for the last half a century. The heavy-ion collision experiments at the Relativistic Heavy Ion Collider (RHIC) in Brookhaven and the Large Hadron Collider (LHC) at CERN give a strong experiment evidences to study such matter on the earth, especially the quark-gluon plasma(QGP) produced in heavy-ion collision experiments. The study of the fundamental properties of the corresponding deconfined state of matter is the broad goal of the ongoing program. Besides, in the noncentral heavy-ion collisions, the QGP are produced with a super strong magnetic field. In the early stages of the collision, the strength of the magnetic field could be estimated [1-4]. However, how strong the magnetic field in the latter stages of the collision when the hot plasma forms and expands is still a puzzle. If it remains relatively strong, the magnetic field can trigger anomalous phenomena, modify the flow of plasma, cause new types of collective modes, and affect the emission of particles. In addition, the large background effects make huge difficulty on the observations of magnetic field from the experiments.

The electromagnetic probes (i.e., photons and leptons) play a unique role in heavy ion collision experiments. Unlike the strongly interacting hadrons, they have long mean-free paths that greatly exceed the size of the fireballs created by the collisions. Thus, they carry invaluable information about the plasma directly to the detectors. Recently, several measurements of electromagnetic emissions were reported by both RHIC and LHC[5-16]. In general, the thermal electromagnetic emission rates have been seen as thermometers of the QGP. In this study, we will introduce the thermal electromagnetic emission rates that can be perfect magnetometers for the hot QGP with a strong background magnetic field.

One has to be argued that, in a vanishing magnetic field case, the leading order photon production is given by the gluon-mediated $2 \to 2$ processes which are linear in the strong coupling constant α_s[17-23]. In strongly magnetized plasma, the photon rate is dominated by the following three single-photon processes: (i) the quark splitting ($q \to q + \gamma$), (ii) the antiquark splitting ($\bar{q} \to \bar{q} + \gamma$), and (iii) the quark-antiquark annihilation ($q+\bar{q} \to \gamma$) which are no longer forbidden by the energy-momentum conservation. And the photon rate is nonzero already at the leading zeroth order in α_s[24-26].

For the dilepton, in a vanishing magnetic field, the thermal radiation from the QGP, the Drell–Yan process, and semileptonic decays of heavy quarks provide the dominant contributions to the dilepton rate in the intermediate range of the dilepton invariant masses. However, the signature effects of the magnetic field are the rate enhancement and strong anisotropy, whose measurements could provide valu-

Received date: 24 Nov. 2023; **Revised date:** 24 Nov. 2023
Foundation item: start-up funding of Jiangsu University(4111190010)
Biography: Xiaozhu Yu(1980–), Zhenjiang, Zhejiang Province, assistant professor, working on condense matter physics and nuclear physics.; E-mail: xzyu@ujs.edu.cn
Corresponding author: E-mail: wangxy@ujs.edu.cn

able bounds on the field strength in the plasma produced by heavy-ion collisions[27].

The main goal of this paper is to introduce the recent theoretical understanding of photon/dilepton emission from a strongly magnetized hot QGP. The corresponding results will reveal a nontrivial anisotropic photon/dilepton emission caused by the background magnetic field for a range of model parameters. As we will argue, such anisotropy carries information about the magnitude of the magnetic field at the early stages of heavy-ion collisions.

2 Anisotropic flow

In noncentral heavy-ion collisions, the anisotropic flow coefficients (v_n) are defined by the following Fourier decomposition of the azimuthal particle distributions[28-29]:

$$E\frac{\mathrm{d}^3N}{\mathrm{d}^3\mathbf{p}} = \frac{1}{2\pi}\frac{\mathrm{d}^2N}{p_T\mathrm{d}p_T\mathrm{d}y}\left(1+2\sum_{n=1}^{\infty}v_n\cos[n(\phi-\Psi_{\mathrm{RP}})]\right), \tag{1}$$

where E is the particle energy, $\mathbf{p}$ is the momentum, p_T is the transverse momentum, ϕ is the azimuthal angle, y is the rapidity, and Ψ_{RP} is the reaction plane angle. By definition,

$$v_n(p_T,y) = \langle\cos[n(\phi-\Psi_{\mathrm{RP}})]\rangle, \tag{2}$$

where the angular brackets denote the average over all particles (or all events, or both) in a given bin of the transverse momentum (p_T) and rapidity (y). Note that the second coefficients in the Fourier decomposition v_2, characterize the elliptic flow.

The direction of the magnetic field in a noncentral collision is (approximately) perpendicular to the reaction plane. In the paper, we assume z axis is the direction of the magnetic field, x-y is the reaction plane and the x axis points along the beam direction. The azimuthal angle ϕ measures the angle between the particle momentum $\mathbf{p}$ and the reaction plane. The particle four-momentum is given by $p^\mu = (p^0, \mathbf{p})$. The transverse components of the particle momentum are given by

$$p_y = p_T\cos(\phi), \quad p_z = p_T\sin(\phi). \tag{3}$$

where $p_T = \sqrt{p_y^2+p_z^2}$ is the magnitude of the transverse momentum.

For photon/dilepton, we assume that the mean free path is larger than the system size so that the particles leave the plasma region without reabsorption. The anisotropy coefficients v_n can be evaluated from the differential distribution of particles as follows:

$$v_n = \frac{1}{\mathcal{R}_0}\int_0^{2\pi}\frac{d^3R}{p_Tdp_Td\phi dy}\cos(n\phi)d\phi, \tag{4}$$

where the normalization factor is given by the particle production rate integrated over the angular coordinate ϕ, i.e.,

$$\mathcal{R}_0 = \frac{d^2R}{p_Tdp_Tdy} = \int_0^{2\pi}\frac{d^3R}{p_Tdp_Tdyd\phi}d\phi. \tag{5}$$

3 Thermal photons in a magnetized QGP

By making use of quantum field theory, the thermal photon production rate can be expressed in terms of the imaginary part of the retarded polarization tensor as follows[30]:

$$p^0\frac{d^3R}{dp_xdp_ydp_z} = -\frac{1}{(2\pi)^3}\frac{\mathrm{Im}\left[\Pi^\mu_\mu(p)\right]}{\exp\left(\frac{p_0}{T}\right)-1}. \tag{6}$$

Because of a quantizing background magnetic field, the quark and antiquark states in the one-loop photon polarization are characterized by the Landau-level quantum numbers, the integer indices n and n'. For simplicity, we will assume that the masses of both light quarks are the same, namely, $m_u = m_d = m = 5$ MeV. The flavor-dependent quark charges are q_f, where $q_u = 2/3e$, $q_d = -1/3e$, and e is the absolute value of the electron charge. We define the modified fine structure constant $\alpha_f = q_f^2/(4\pi)$ for different flavors of quarks. $N_c = 3$ is the number of colors, T is the temperature of the system and n_F is the Fermi-Dirac distribution function.

The imaginary part of the (Lorentz-contracted) polarization tensor in the leading order with a background magnetic field can be written as follows[26]:

$$\begin{aligned}\mathrm{Im}\left[\Pi^\mu_{R,\mu}\right] = &\sum_{f=u,d}\frac{N_c\alpha_f}{2\pi l_f^4}\sum_{n>n'}^{\infty}g(n,n')\\ &\frac{\left[\theta\left(p_{-,f}^2-p_0^2+p_3^2\right)-\theta\left(p_0^2-p_3^2-p_{+,f}^2\right)\right]}{\sqrt{[p_{-,f}^2+p_z^2-p_0^2][p_{+,f}^2+p_z^2-p_0^2]}}\mathcal{F}^f_{n,n'}\\ -&\sum_{f=u,d}\frac{N_c\alpha_f}{4\pi l_f^4}\sum_{n=0}^{\infty}\frac{g_0(n)\theta\left(p_0^2-p_z^2-p_{+,f}^2\right)}{\sqrt{(p_0^2-p_z^2)(p_0^2-p_z^2-p_{+,f}^2]}}\mathcal{F}^f_{n,n},\end{aligned} \tag{7}$$

where $\theta(x)$ is the Heaviside step function, the transverse momentum thresholds are given by

$$p_{\pm,f} = \left|\sqrt{m^2+2n|q_fB|}\pm\sqrt{m^2+2n'|q_fB|}\right|. \tag{8}$$

We also used the following shorthand notations:

$$\begin{aligned} g(n,n') &= 2-\sum_{s_1,s_2=\pm} n_F\left(\frac{p_0}{2}+s_1\frac{p_0(n-n')|q_fB|}{p_0^2-p_z^2}\right. \\ &+ \left. s_2\frac{|p_z|}{2(p_0^2-p_z^2)}\sqrt{\left(p_0^2-p_z^2-p_{-,f}^2\right)\left(p_0^2-p_z^2-p_{+,f}^2\right)}\right), \\ g_0(n) &= g(n,n), \end{aligned} \tag{9}$$

and the explicit form of the corresponding function reads

$$\begin{aligned} \mathcal{F}^f_{n,n'}(\xi) &= 8\pi\left(n+n'+m^2\ell_f^2\right)\left[\mathcal{I}^{n,n'}_{0,f}(\xi)+\mathcal{I}^{n-1,n'-1}_{0,f}(\xi)\right] \\ &+8\pi\left[\frac{\left(p_0^2-\mathbf{p}^2\right)\ell_f^2}{2}-(n+n')\right]\left[\mathcal{I}^{n,n'-1}_{0,f}(\xi)+\mathcal{I}^{n-1,n'}_{0,f}(\xi)\right], \end{aligned} \tag{10}$$

where functions $\mathcal{I}^{n,n'}_{0,f}(\xi)$ are defined in terms of the generalized Laguerre polynomials[31] as follows:

$$\mathcal{I}^{n,n'}_{0,f}(\xi) = (-1)^{n+n'}e^{-\xi}L_n^{n'-n}(\xi)\,L_{n'}^{n-n'}(\xi), \tag{11}$$

$\xi=(k_\perp\ell_f)^2/2$ and the flavor-specific magnetic length $\ell_f = 1/\sqrt{|q_fB|}$.

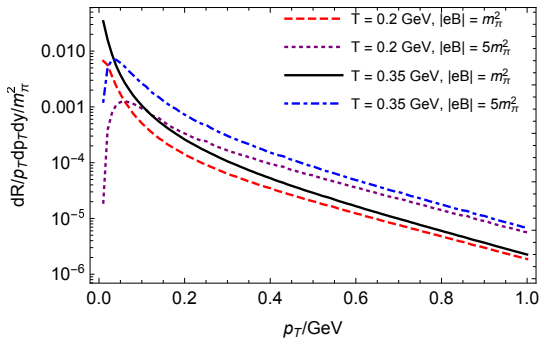

Fig. 1 The integrated photon production rate as a function as a function of the transverse momentum p_T for two different magnetic field: $|eB|=m_\pi^2$, $|eB|=5m_\pi^2$ and two different temperatures: $T=200$ MeV, $T=350$ MeV[24,26]

.

The total rate integrated over the angular coordinate are plotted in Fig. 1 for both two different magnetic fields and two different temperatures:(1) $|eB|=m_\pi^2$, $T=200$ MeV(red dashed line), (2) $|eB|=5m_\pi^2$, $T=350$ MeV(purple dotted line), (3) $|eB|=m_\pi^2$, $T=350$ MeV(black solid line), (4) $|eB|=5m_\pi^2$, $T=350$ MeV(Blue dot-dashed line). In the case of the stronger field, $|eB|=5m_\pi^2$, there are indeed well-resolved peaks in the photon production rate at $p_T\simeq 0.06$ GeV when $T=0.2$ GeV and at $p_T\simeq 0.04$ GeV when $T=0.35$ GeV. For each case, the transverse momenta were taken in the range between 0.01 GeV to 1 GeV with discretization step 0.01 GeV, and the azimuthal angle was

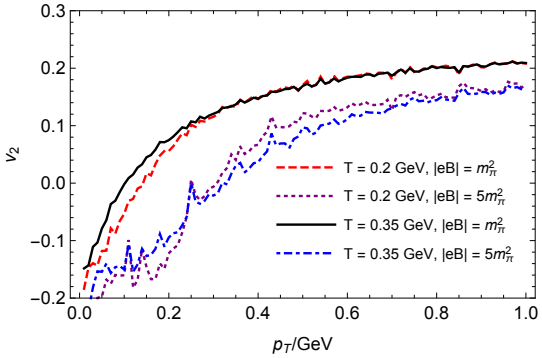

Fig. 2 Ellipticity of the photon production as a function of the transverse momentum p_T for two different magnetic fields: $|eB|=m_\pi^2$, $|eB|=5m_\pi^2$ and two different temperatures: $T=200$ MeV, $T=350$ MeV[24,26]

.

considering the range between $10^{-4}\frac{\pi}{2}$ and $\frac{\pi}{2}-10^{-4}\frac{\pi}{2}$ with the discretization step $10^{-3}\frac{\pi}{2}$.

As argued in Ref.[26], there also should have similar peaks appear in the case of weaker fields. The existence of such maxima is a necessary consequence of the Landau-level quantization of quark states in a strongly magnetized plasma. However, because of the numerical calculation difficulties at tiny p_T, the peak is not showing here. The maxima are larger when the temperature is higher and the magnetic field is weaker. In addition, when the transverse momentum increases further, the photon production rate starts to decrease quickly. The higher temperature and larger magnetic field induced a higher rate at larger p_T.

To better understand the role of the magnetic field on the direct photon emission from hot quark-gluon plasma, we show the plot of the ellipticity v_2 dependence on the transverse momentum in Fig. 2. For all the physics parameters we are plotting here, we found in all the cases we have the following feature. At large p_T, the ellipticity reaches and saturates at a relatively large positive value, i.e, $v_{2,max}\simeq 0.2$. At small p_T regime $p_T\lesssim\sqrt{|eB|}$, the ellipticity become negative. The sign of v_2 changes at around $p_T\simeq\sqrt{|eB|}$. The corresponding results mean, the emission rate at small values of p_T has an overall tendency to peak at $\phi=\frac{\pi}{2}$, i.e., in the direction perpendicular to the reaction plane. When the value of p_T is larger than about $\sqrt{|eB|}$, the emission tends to be highest at $\phi=0$, i.e., in the direction along the reaction plane. Such anisotropic emission is caused by a strong magnetic field and has nothing to do with the hydrodynamic behavior of the quark-gluon plasma(see Ref.[24] for details).

4 Dileptons in a magnetized QGP

The dilepton rate is given by[32]

$$dR_{l\bar{l}} = 2\pi e^2 e^{-\beta k_0} L_{\mu\nu}(Q_1, Q_2)\rho^{\mu\nu}(k_0, \mathbf{k}) \frac{d^3\mathbf{q}_1}{(2\pi)^3 E_1} \frac{d^3\mathbf{q}_2}{(2\pi)^3 E_2}, \tag{12}$$

where the three-momenta and energies of the two leptons are denoted by $\mathbf{q}_i$ and E_i with $i = 1, 2$, respectively. One should notice here, to distinguish with photon in previous section, we use $k^\mu = (k_0, \mathbf{k})$ as the four-momenta of the dilepton in this section. To the leading linear order in the electromagnetic coupling constant, the electromagnetic spectral function $\rho^{\mu\nu}(k_0, \mathbf{k})$ is expressed in terms of the imaginary part of the photon polarization tensor as follows:

$$\rho^{\mu\nu}\left(k_0, \mathbf{k}\right) = -\frac{1}{\pi} \frac{e^{\beta k_0}}{e^{\beta k_0} - 1} \frac{\mathrm{Im}\left[\Pi^{\mu\nu}\left(k_0, \mathbf{k}\right)\right]}{K^4}. \tag{13}$$

In Eq. (12), the leptonic tensor for the final plane-wave states has the following explicit form:

$$L_{\mu\nu}(Q_1, Q_2) = \frac{1}{4} \sum_{\text{spins}} \mathrm{tr}\left[\bar{u}\left(Q_2\right)\gamma_\mu v\left(Q_1\right)\bar{v}\left(Q_1\right)\gamma_\nu u\left(Q_2\right)\right], \tag{14}$$

By using the explicit form of the leptonic tensor and setting the lepton masses m_l to zero, the corresponding differential rate reads[32]

$$\frac{dR_{l\bar{l}}}{d^4K} = \frac{\alpha}{12\pi^4} \frac{n_B\left(p_0\right)}{M^2} \mathrm{Im}\left[\Pi^\mu_\mu\left(k_0, \mathbf{k}\right)\right], \tag{15}$$

where $\alpha \equiv e^2/(4\pi) = 1/137$ is the fine structure constant and $n_B(k_0) = (e^{k_0/T} - 1)^{-1}$ is the Bose-Einstein distribution function. $M^2 = K^2 = k^2 \equiv k_0^2 - k_\perp^2 - k_z^2$ is the square of the invariant mass of the lepton pair. By definition, $k_\perp = \sqrt{k_x^2 + k_y^2}$ is the magnitude of the momentum component perpendicular to the magnetic field. Note that $d^4K = MdMk_T dk_T dyd\phi$, where $p_T = \sqrt{k_y^2 + k_z^2}$ is the transverse momentum (with respect to the beam direction) and $y = \frac{1}{2}\ln\frac{k_0 + k_x}{k_0 - k_x}$ is the rapidity.

After applying the imaginary part of the Lorentz-contracted photon polarization tensor in Eq. (7), the final result reads

$$\begin{aligned}
\frac{dR_{l\bar{l}}}{d^4K} = {} & \frac{\alpha^2 N_c}{48\pi^5} \frac{n_B(\Omega)}{M^2} \sum_{f=u,d} \frac{q_f^2}{\ell_f^4} \\
& \Bigg[\sum_{n=0}^{\infty} \frac{g_0(n)\theta\left(\sqrt{M^2 + k_\perp^2} - k_{+,f}\right)}{\sqrt{(M^2 + k_\perp^2)\left[M^2 + k_\perp^2 - k_{+,f}^2\right]}} \mathcal{F}^f_{n,n}(\xi) \\
& - 2\sum_{n>n'}^{\infty} \frac{g(n,n')\theta\left(k_{-,f} - \sqrt{M^2 + k_\perp^2}\right)\mathcal{F}^f_{n,n'}(\xi)}{\sqrt{\left[k_{-,f}^2 - (M^2 + k_\perp^2)\right]\left[k_{+,f}^2 - (M^2 + k_\perp^2)\right]}} \\
& + 2\sum_{n>n'}^{\infty} \frac{g(n,n')\theta\left(\sqrt{M^2 + k_\perp^2} - k_{+,f}\right)\mathcal{F}^f_{n,n'}(\xi)}{\sqrt{\left[k_{-,f}^2 - (M^2 + k_\perp^2)\right]\left[k_{+,f}^2 - (M^2 + k_\perp^2)\right]}} \Bigg].
\end{aligned} \tag{16}$$

In addition, it is useful to compare the results with the corresponding rate in the zero-field limit. In the Born approximation, the rate is given by[33]

$$\frac{dR_{l\bar{l},\text{Born}}}{d^4k} = \frac{5\alpha^2 T}{18\pi^4|\boldsymbol{k}|} n_B(k_0) \ln\left(\frac{\cosh\frac{k_0 + |\boldsymbol{k}|}{4T}}{\cosh\frac{k_0 - |\boldsymbol{k}|}{4T}}\right), \tag{17}$$

where the massless quarks and leptons are assumed.

The dependence of the rate on the invariant mass is presented in Fig. 3. The corresponding data was calculated for the whole range of invariant masses between $M_{\min} = 0.02$ GeV and $M_{\max} = 1$ GeV, using the discretization step $\Delta M = 0.01$ GeV. Individual panels show the results for two representative choices of temperature, i.e., $T = 0.2$ GeV and $T = 0.35$ GeV, and two values of the magnetic field, i.e., $|eB| = m_\pi^2$ and $|eB| = 5m_\pi^2$. Each panel contains the rates for the same set of fixed values of the transverse momenta, i.e., $k_T = 0$ (black), $k_T = 0.1$ GeV (blue), $k_T = 0.2$ GeV (orange), $k_T = 0.5$ GeV (green), and $k_T = 1$ GeV (red). For comparison, we also show the zero-field Born rate (dashed lines).

By comparing the overall profiles of dilepton rates in a strongly magnetized plasma with the benchmark zero-field Born rate, the rates at $B \neq 0$ remain about the same on average as those at $B = 0$ when the invariant mass is sufficiently large, i.e., $M \gtrsim \sqrt{|eB|}$. On the other hand, the magnetic field has a dramatic effect on the dilepton production in the region of small invariant masses, i.e., $M \lesssim \sqrt{|eB|}$, where the rates are strongly enhanced. As seen in Fig. 3, the rate can increase by several orders of magnitude when M de-

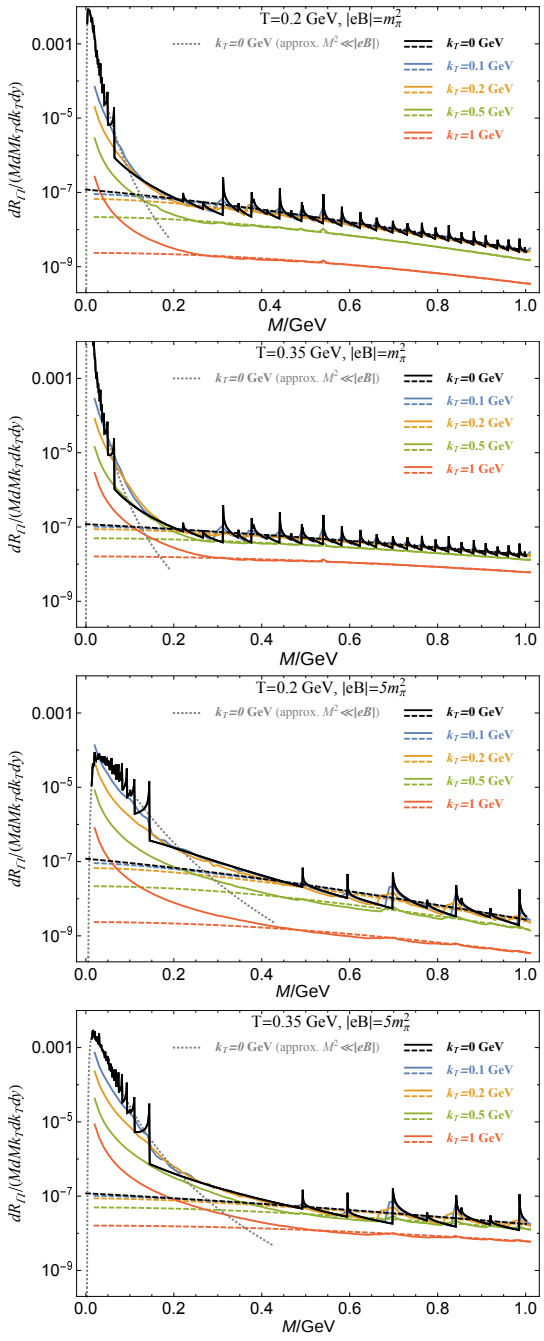

Fig. 3 The integrated dilepton rate as a function of the dilepton invariant mass M for several fixed values of the transverse momentum $k_T = 0, 0.1, 0.2, 0.5, 1$ GeV, two values of the temperature, i.e., $T = 0.2$ GeV and $T = 0.35$ GeV, and two values of the magnetic field, i.e., $|eB| = m_\pi^2$ and $|eB| = 5m_\pi^2$). For comparison, the dashed lines represent the zero-field Born rate and the gray dotted lines show the approximate rate at $k_T = 0$ and $M \ll \sqrt{|eB|}$ [27].

creases only by half. The dilepton rate is on-average a decreasing function of the invariant mass M. Generically, the rate in the magnetized QGP approaches the zero-field Born result (17) when the invariant mass is sufficiently large (i.e., $M \gg \sqrt{|eB|}$). By comparing the plots in Fig. 3 for different values of the transverse momenta, we see that the dilepton rate tends to decrease with increasing k_T. As one can verify, the suppression of the rate at large M or k_T (or both) comes primarily from the overall Bose distribution function $n_B(\Omega)$ in Eq. (16).

The dependence of the ellipticity parameter v_2 on the dilepton invariant mass M is shown in Fig. 4.In the case of small invariant masses, $M \lesssim \sqrt{|eB|}$, there is a clear tendency of v_2 to become positive. The latter is particularly well pronounced at large k_T, which is analogous to the photon emission. Such a behavior is because the angular dependence of the rate are systematically larger for the azimuthal directions near $\phi \approx 0$ (in the reaction plane) and systematically smaller for $\phi \approx \pi/2$ (out of the reaction plane). On the other hand, the value of the ellipticity parameter v_2 for the dilepton rate at small invariant masses, $M \lesssim \sqrt{|eB|}$, and large transverse momenta is positive.

The overall ellipticity is harder to discern from the data at small values of the transverse momenta, i.e., $k_T = 0.1$ GeV (blue lines) and $k_T = 0.2$ GeV (orange lines). For sufficiently small invariant masses, $M \lesssim \sqrt{|eB|}$, the ellipticity parameter appears to be generally nonvanishing. However, as seen from Fig. 4, its sign may change from being positive at intermediate values of M (i.e., $M \simeq \sqrt{|eB|}$), to being negative at sufficiently small values of M (i.e., $M \ll \sqrt{|eB|}$). This is particularly clear in the case of the stronger magnetic field $|eB| = 5m_\pi^2$. It should be also noted that the average ellipticity parameter v_2 is consistent with zero for sufficiently large invariant masses, $M \gtrsim \sqrt{|eB|}$.

5 Summary

The electromagnetic probes in relativistic heavy-ion collisions provide an ideal environment to study the properties of QCD matter under extreme conditions. By using the Landau-level representation for the imaginary part of the photon polarization tensor, we got an explicit expression for the photon/dilepton emission rate from a hot QGP in a quantizing background magnetic field.

For the photon emission from a strongly magnetized hot quark-gluon plasma, there is a nonzero ellipticity coefficient

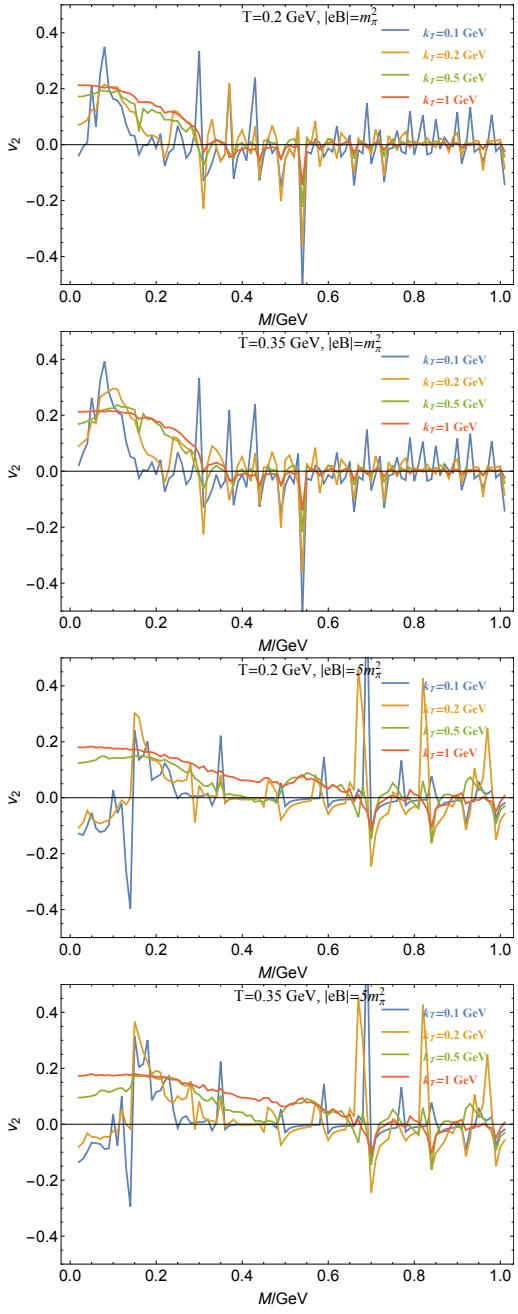

Fig. 4　The dilepton emission ellipticity as a function of the dilepton invariant mass M for two temperatures, i.e., $T = 0.2$ GeV and $T = 0.35$ GeV, and two magnetic fields, i.e., $|eB| = m_\pi^2$ and $|eB| = 5m_\pi^2$). Each panel shows the results for four fixed transverse momenta, i.e., $k_T = 0.1$ GeV (blue), $k_T = 0.2$ GeV (orange), $k_T = 0.5$ GeV (green), and $k_T = 1$ GeV (red)[27].

v_2 that depends on the transverse momentum. v_2 is negative at small momenta, $p_T \lesssim \sqrt{|eB|}$, and positive at large momenta, $k_T \gtrsim \sqrt{|eB|}$. While the ellipticity coefficient v_2 is an overall growing function of p_T, it reaches a relatively high positive value $v_{2,max} \simeq 0.2$ at large p_T. One of the most exciting thing is the negative value of v_2 at small p_T, this result differs from the one in any hydrodynamic or transport calculations that predict positive v_2 for any p_T [34]. If such negative value could be measured, this definitely an evidence of the existent magnetic field in the QGP plasma.

For dilepton, the anisotropy is pronounced the most in the regime of small values of the dilepton invariant mass $M \lesssim \sqrt{|eB|}$. When the transverse momenta are large, the ellipticity parameter v_2 tends to be positive and large. For small transverse momenta, the ellipticity parameter v_2 may still remain nonzero in general. However, its sign gradually changes from being positive at intermediate values of M (i.e., $M \simeq \sqrt{|eB|}$) to being negative at small M (i.e., $M \ll \sqrt{|eB|}$). Under optimal conditions, we find that the magnitude of v_2 could be as large as 0.2. If such large values are measured in an experiment, they will most likely indicate the presence of a nonzero magnetic field in the QGP plasma.

Besides, the background field strongly enhances the rate at small values of the dilepton invariant mass ($M \lesssim \sqrt{|eB|}$). At large values of the invariant mass ($M \gtrsim \sqrt{|eB|}$), of course, the role of the magnetic fields decreases, and the results gradually approach the isotropic zero-field Born rate. Such significant enhancement of the integrated dilepton rate at small invariant masses is a unique signature of a nonzero background magnetic field. Thus, measuring the corresponding rate at $M \lesssim 0.2$ GeV, for example, could provide sufficient information to confirm or rule out the fields of order $|eB| \simeq m_\pi^2$ in relativistic heavy-ion collisions.

6　Acknowledgments

The work of X.W. is supported by the start-up funding No. 4111190010 of Jiangsu University.

References

[1] SKOKOV V, ILLARIONOV A, TONEEV V, Int. J. Mod. Phys. A **24**, 5925 (2009). doi:10.1142/S0217751X09047570

[2] DENG W, HUANG X, Phys. Rev. C **85**, 044907 (2012). doi:10.1103/PhysRevC.85.044907

[3] TUCHIN K, Phys. Rev. C **93**, 014905 (2016). doi:10.1103/PhysRevC.93.014905

[4] GUO X, LIAO J, WANG E, Sci. Rep. **10**, 2196 (2020). doi:10.1038/s41598-020-59129-6
[5] ADARE A, *et al.* (PHENIX Collaboration), Phys. Rev. Lett. **109**, 122302 (2012). doi:10.1103/PhysRevLett.109.122302
[6] ADARE A, *et al.* (PHENIX Collaboration), Phys. Rev. C **94**, 064901 (2016). doi:10.1103/PhysRevC.94.064901
[7] ACHARYA S, *et al.* (ALICE Collaboration), Phys. Lett. B **789**, 308 (2019). doi:10.1016/j.physletb.2018.11.039
[8] ADAMCZYK L, *et al.* (STAR Collaboration), Phys. Rev. C **92**, 024912 (2015). doi:10.1103/PhysRevC.92.024912
[9] SECK F (STAR Collaboration), Nucl. Phys. **A1005**, 122005 (2021). doi:10.1016/j.nuclphysa.2020.122005
[10] ACHARYA S, *et al.* (ALICE Collaboration), Phys. Rev. Lett. **127**, 042302 (2021). doi:10.1103/PhysRevLett.127.042302
[11] ADAM J, *et al.* (STAR Collaboration), Phys. Rev. Lett. **121**, 132301 (2018). doi:10.1103/PhysRevLett.121.132301
[12] ADAM J, *et al.* (STAR Collaboration), arXiv:1810.10159 [nucl-ex].
[13] ADARE A, *et al.* (PHENIX Collaboration), Phys. Rev. C **93**, 014904 (2016). doi:10.1103/PhysRevC.93.014904
[14] ADAMCZYK L, *et al.* (STAR Collaboration), Phys. Lett. B **750**, 64 (2015). doi:10.1016/j.physletb.2015.08.044
[15] ADARE A, *et al.* (PHENIX Collaboration), Phys. Rev. C **81**, 034911 (2010). doi:10.1103/PhysRevC.81.034911
[16] ACHARYA S, *et al.* (ALICE Collaboration), Phys. Rev. C **99**, 024002 (2019). doi:10.1103/PhysRevC.99.024002
[17] KAPUSTA J, LICHARD P, SEIBERT D, Phys. Rev. D **44**, 2774 (1991); doi:10.1103/PhysRevD.44.2774 **47**, 4171(E) (1993). doi:10.1103/PhysRevD.47.4171
[18] BAIER R, NAKKAGAWA H, NIEGAWA A, REDLICH K, Z. Phys. C **53**, 433 (1992). doi:10.1007/BF01625902
[19] AURENCHE P, GELIS F, ZARAKET H, KOBES R, Phys. Rev. D **58**, 085003 (1998). doi:10.1103/PhysRevD.58.085003
[20] STEFFEN F, THOMA M, Phys. Lett. B **510**, 98 (2001). doi:10.1016/S0370-2693(01)00525-1
[21] ARNOLD P, MOORE G, YAFFE L, J. High Energy Phys. **11** (2001) 057. doi:10.1088/1126-6708/2001/11/057
[22] ARNOLD P, MOORE G, YAFFE L, J. High Energy Phys. **12** (2001) 009. doi:10.1088/1126-6708/2001/12/009
[23] GHIGLIERI J, HONG J, KURKELA A, LU E, MOORE G, TEANEY D, J. High Energy Phys. **05** (2013) 010. doi:10.1007/JHEP05(2013)010
[24] WANG X, SHOVKOVY I, YU L, HUANG M, Phys. Rev. D **102**, no.7, 076010 (2020). doi:10.1103/PhysRevD.102.076010
[25] WANG X, SHOVKOVY I, Phys. Rev. D **104**, no.5, 056017 (2021). doi:10.1103/PhysRevD.104.056017
[26] WANG X, SHOVKOVY I, Eur. Phys. J. C **81**, no.10, 901 (2021). doi:10.1140/epjc/s10052-021-09650-3
[27] WANG X, SHOVKOVY I, Phys. Rev. D **106**, no.3, 036014 (2022). doi:10.1103/PhysRevD.106.036014
[28] VOSHIN S, ZHANG Y, Z. Phys. C **70**, 665 (1996). doi:10.1007/s002880050141
[29] POSKANZER A, VOLOSHIN S, Phys. Rev. C **58**, 1671 (1998). doi:10.1103/PhysRevC.58.1671
[30] KAPUSTA J, GALE C, *Finite-temperature field theory: Principles and applications*, (Cambridge University Press, Cambridge, England, 2006), p. 330.
[31] Gradshtein I, Ryzhik I, *Tables of Integrals, Series, and Products* (Academic Press, Orlando, 1980).
[32] WELDON H, Phys. Rev. D **42**, 2384 (1990). doi:10.1103/PhysRevD.42.2384
[33] CLEYMANS J, FINGBERG J, REDLICH K, Phys. Rev. D **35**, 2153 (1987). doi:10.1103/PhysRevD.35.2153
[34] BLAU D, PERESUNK D, Particles **6**, no.1, 173-187 (2023). doi:10.3390/particles6010009

磁化等离子体中的非均匀辐射

俞笑竹[1]，王昕杨[1]

(1. 江苏大学物理系，镇江 212013;)

摘要：通过研究了有限温度下强磁化夸克胶子等离子体的极化效应发现，背景磁场对光子和双轻子发射率有很强的影响。它不仅影响总发射率，还影响角度相关性。特别是，朗道能级量子化导致光子/双轻子椭圆度系数对横向动量的非平凡动量依赖性。光子和双轻子产生过程的各向异性也可以作为对磁场的测量一种重要的间接手段。

关键词：重离子碰撞；电磁探针；强磁场；有限温度场论；

收稿日期：2023-11-24；　**修改日期：**2023-11-24

基金项目：江苏大学启动经费 (4111190010)

通信作者：王昕杨，E-mail: wangxy@ujs.edu.cn